ChemComm

Accepted Manuscript

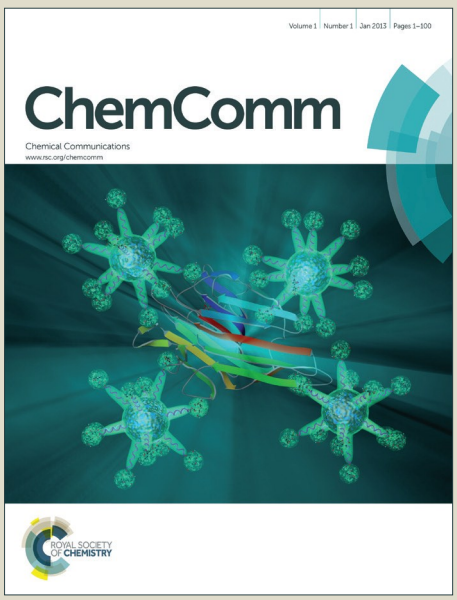

ROYAL SOCIETY OF CHEMISTRY

www.rsc.org/chemcomm

Journal Name

RSCPublishing

COMMUNICATION

Two-Step Naked-Eye Detection of a Lectin by Hierarchical Organization of Soft Nanotubes into Liquid Crystal and Gel Phases

Cite this: DOI: 10.1039/x0xx00000x

Received ooth January 2012,
Accepted ooth January 2012

DOI: 10.1039/x0xx00000x

www.rsc.org/

Naohiro Kameta,[a*] Mitsutoshi Masuda[a] and Toshimi Shimizu[b]

Depending on the concentration of a lectin analyte, supramolecular soft nanotubes, bearing recognition sites immobilized on the outer surface through ethylene glycol chains, hierarchically organized into naked-eye-detectable liquid crystals and hydrogels.

Methods for the naked-eye detection of biomolecules by using nanoparticles and nanofibers have attracted much attention in biology and medicine because such methods can be used for on-site analysis and quick diagnosis without analytical instruments. For example, gold nanoparticles that exhibit the plasmon resonance effect are widely used for colorimetric detection of DNA and proteins.[1] Supramolecular hydrogels, which consist of a nanofiber network self-assembled from organic gelators, also have great potential for biosensing.[2] Macroscopic changes of supramolecular hydrogels, such as sol–gel transitions in response to specific interactions and selective reactions of the gelators with target biomolecules and related compounds, are easily detected by the naked eye and are especially useful for qualitative analysis. Introduction of rationally designed absorbing or fluorescent groups into the gelators in advance allows the construction of supramolecular hydrogels in which the sol–gel transitions are accompanied by a color change. Such systems can be used for both qualitative and quantitative analysis. Recently, we and other researchers found that soft nanotubes,[3] which are formed by self-assembly of amphiphilic molecules in water, often hierarchically organize into hydrogels and liquid crystals, in which the soft nanotubes have network and aligned structures, respectively.[4]

Herein we describe soft nanotubes that exhibit two continuous macroscale phases, a hydrogel and a liquid crystal, depending on the concentration of a lectin analyte. We investigated how the length of the ethylene glycol chains that anchor the lectin-recognition sites to the outer surface of the nanotubes affected the efficacy of this method for qualitative and quantitative naked-eye detection of the lectin.

Concanavalin A (Con A), which has high affinities for mannose and glucose, was selected as the target lectin. As previously reported,[5] self-assembly of amphiphiles **1** produces molecular monolayer nanotubes (hereafter referred to as 1-nanotubes) with an inner diameter of 8 nm, a wall thickness of 3 nm, and a length of up to several micrometers. The 1-nanotubes do not recognize Con A (as described later), even though their outer surface is covered with the glucose headgroups of **1**.

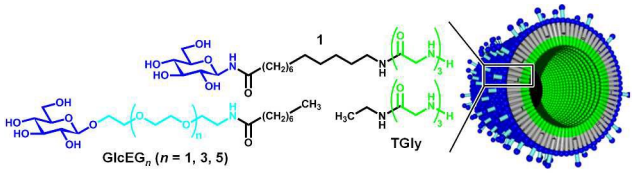

Fig. 1 A molecular monolayer nanotube (GlcEG$_n$-nanotube) composed of **1**, TGly (10 mol% against **1**), and GlcEG$_n$ (10 mol% against **1**).

We newly synthesized glucose derivatives GlcEG$_n$ (n = 1, 3, and 5) as recognition sites for Con A (Fig. 1, Scheme S1, ESI) and selectively located them on the outer surface of the nanotubes by means of a two-step self-assembly process. First, binary self-assembly of **1** and a triglycine derivative (TGly) was carried out as follows: A mixture of **1** (1.0 mg, 1.8 μmol) and TGly (43.2 μg, 0.20 μmol) was dispersed in pure water (1 ml) under reflux conditions, and then the hot solution was gradually cooled to room temperature. Transmission electron microscopy (TEM) revealed that the binary self-assembly process gave nanotubes (hereafter referred to as 2-nanotubes) that were similar to the 1-nanotubes in terms of the inner diameter, wall thickness, and length (Fig. S1, ESI). The differential scanning calorimetry profile of the 2-nanotube had single endothermic peak corresponding to a thermal phase transition of the monolayer membrane (Fig. S2, ESI), supporting the conclusion that the 2-nanotube is composed of both **1** and TGly, even though the common molecular part is the triglycine moiety. The lowering of the thermal phase-transition temperature ($T_{g\text{-}l}$ = 52 °C) of the 2-nanotubes in water comparing with that ($T_{g\text{-}l}$ = 67 °C) of the 1-nanotube is ascribable to void spaces in the molecular packing due to the fact that TGly lacks the long alkyl chain and the glucose headgroup of **1**.

In the second step of the self-assembly process, 2-nanotubes (**1** = 1.8 μmol, TGly = 0.20 μmol) were heated with GlcEG$_n$ (0.20 μmol) at around the $T_{g\text{-}l}$ temperature of the 2-nanotubes (52 °C) in water (1 ml). After the heating process, we confirmed neither morphological changes nor the formation of other structures by transmittance electron microscopic (TEM) observations (Fig. 2a, Fig. S1, ESI), although the GlcEG$_n$ molecules themselves self-assembled in water

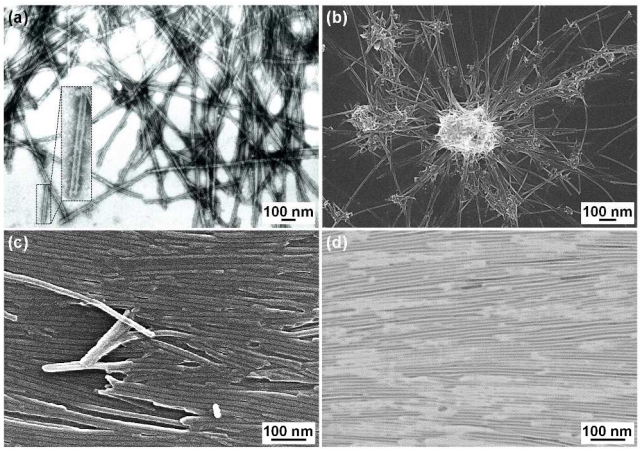

Fig. 2 (a) TEM image of $GlcEG_3$-nanotubes. (b) SEM image of a xerogel of $GlcEG_3$-nanotubes complexed with Con A. (c) SEM and (d) TEM images of a liquid crystal in the dry state of $GlcEG_3$-nanotubes complexed with Con A. The hollow cylinders of the nanotubes in the TEM images were visualized with phosphotungstate as a negative staining reagent.

to form helical nanofibers with a uniform 10-nm width (Fig. S3, ESI). The $T_{g\text{-}l}$ value of the nanotubes formed from **1**, TGly, and $GlcEG_n$ (hereafter referred to as $GlcEG_n$-nanotubes) was 65–67 °C, which suggests that $GlcEG_n$ molecules filled the void spaces within the molecular packing structure of the 2-nanotubes (Fig. S2, ESI). IR spectroscopy supported the molecular packing of **1**, TGly, and $GlcEG_n$ in the $GlcEG_n$-nanotubes, in which TGly forms polyglycine-II-type hydrogen bond network[5] with the trigylcine moiety of **1**, and $GlcEG_n$ never disorder the lateral chain packing of the oligomethylene spacer of **1** assignable to a triclinic parallel type[5] (Fig. S4, Table S1, ESI). All the results indicate that the glucose moiety bonded to the ethylene glycol chain in $GlcEG_n$ was located only on the outer surface of the nanotubes (Fig. 1).

The three types of $GlcEG_n$-nanotubes, which had high axial ratios (>300, axial ratio = length/outer diameter), and the 1-nanotubes form clear dispersions in water (1.1–1.2 mg/1 ml) at pH 7.6 (Fig. 3). The good dispersibility of these nanotubes was due both to the hydrophilicity of the glucose headgroups of **1** on the outer surface and to the negative zeta potentials of the nanotubes at pH 6–8 (Fig. S5, ESI), resulting from adsorption of OH^- groups on the glucose headgroups of **1**.[6] We also confirmed that nonspecific adsorption of Con A on the nanotubes is negligible, owing to electrostatic repulsion between the nanotubes and Con A, which is negatively charged at pH 7.6 (isoelectronic point, pI = 6.3).

Upon addition of Con A (5–100 nmol), the aqueous dispersion of 1-nanotubes (1.0 mg/ml, **1** = 1.8 μmol) remained clear (Fig. 3a), whereas the appearance of the $GlcEG_n$-nanotube dispersions (1.1–1.2 mg/ml, **1** = 1.8 μmol, TGly and $GlcEG_n$ = 0.2 μmol) showed various changes depending on the value of n (Fig. 3b–d). The clear aqueous dispersion of 1-nanotubes and Con A was filtered through a 0.2-μm-pore-size membrane. UV–vis and IR spectroscopic measurements showed that the recovered 1-nanotubes contained no Con A, indicating that the glucose headgroups of **1** on the outer surface of the 1-nanotubes do not bind Con A. Sato et al. reported that a 100%-density maltoside monolayer self-assembled on a gold substrate is unsuitable for Con A detection, whereas a 10%-density maltoside surface can effectively detect Con A.[7] Dense molecular packing of **1** within the monolayer membrane of the 1-nanotubes likely prohibited Con A from accessing and binding to the glucose headgroups. For the same reason, the binding ability of the glucose headgroups of **1** in the $GlcEG_n$-nanotubes must also be very poor.

In contrast, the $GlcEG_n$ molecules anchored to the outer surface

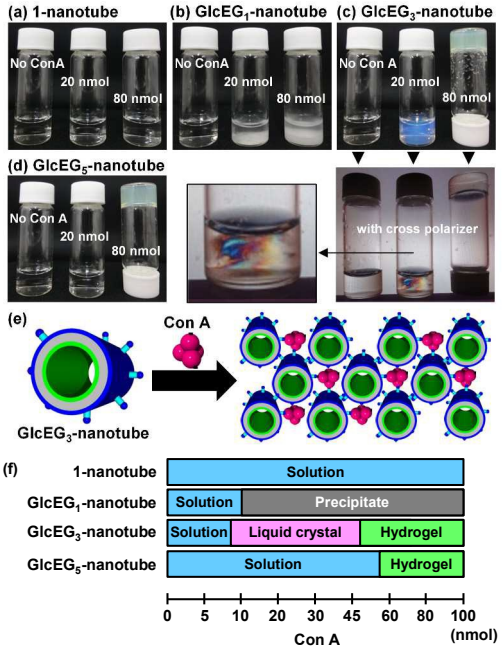

Fig. 3 Photographs of nanotube dispersions (1 ml) in the presence and absence of Con A (= 0, 20, or 80 nmol) at pH 7.6, [NaCl] = 10 mM: (a) 1-nanotube (**1** = 1.8 μmol) and (b,c,d) $GlcEG_n$-nanotubes (**1** = 1.8 μmol, TGly = 0.2 μmol, $GlcEG_n$ = 0.2 μmol). (e) Side-by-side alignment of $GlcEG_3$-nanotubes complexed with Con A. (f) Responsiveness of 1-nanotube and $GlcEG_n$-nanotubes dispersions toward different concentrations of Con A.

of the $GlcEG_n$-nanotubes were able to function as binding sites for Con A. Association constants β (M^{-1}) for the interactions between the $GlcEG_1$-, $GlcEG_2$-, and $GlcEG_3$-nanotubes and Con A were calculated to be 5.9×10^2, 1.9×10^3, and 1.2×10^3, respectively (Fig. S6, ESI), and these values are comparable to that (8.0×10^2) for the association between glucose and Con A.[8] The smaller β value of the $GlcEG_1$-nanotube is attributable to the restricted flexibility of the glucose moiety resulting from the short ethylene glycol chain in $GlcEG_1$.

The appearance of the $GlcEG_3$-nanotube dispersion was remarkably influenced by the Con A concentration. Upon addition of Con A at a relatively high concentration, the $GlcEG_3$-nanotube dispersion quickly transformed to a hydrogel (Fig. 3c, Con A = 80 nmol). Scanning electron microscopy (SEM) observation of the lyophilized hydrogel (xerogel) showed a network of $GlcEG_3$-nanotubes (Fig. 2b). Because Con A has four affinity pockets for glucose, it acted as a cross-linker and promoted formation of the $GlcEG_3$-nanotube network. At a relatively low concentration of Con A, the $GlcEG_3$-nanotube dispersion showed bluish color owing to Rayleigh scattering (Fig. 3c, Con A = 20 nmol). Birefringence was observed under crossed polarizers, indicating a lyotropic liquid crystal formation. SEM and TEM observations of the liquid crystal in the dry state revealed side-by-side alignment of the $GlcEG_3$-nanotubes (Fig. 2c,d and Fig. S7, ESI), which is obviously different from the random orientation of the $GlcEG_n$-nanotubes in dispersions without Con A and the network structure of the $GlcEG_3$-nanotube hydrogels with Con A. These results suggest that $GlcEG_3$-nanotubes form a nematic liquid crystal (Fig. 3c,e). Electrostatic repulsion among phospholipid nanotubes or bipolar-lipid nanotubes is reported to be an important factor for the formation of nematic liquid crystals.[4a,9] The zeta potential of the $GlcEG_3$-nanotubes was estimated to be about –53 mV at pH 7.6 (Fig. S5, ESI). Because Con A is negatively charged at pH 7.6, even the complexed Con A,

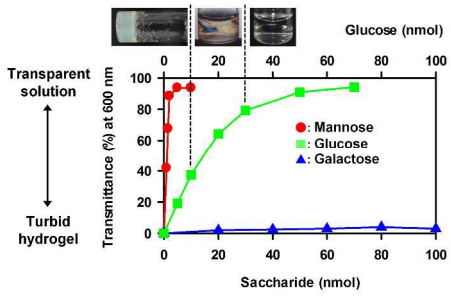

Fig. 4 Saccharide responsiveness of the hydrogel consisting of $GlcEG_3$-nanotubes (1.1 mg/ 1 ml, **1** = 1.8 μmol, TGly = 0.2 μmol, $GlcEG_3$ = 0.2 μmol) complexed with Con A (= 60 nmol), at pH 7.6, [NaCl] = 10 mM.

which acts as the cross linker and locates at the interface of the $GlcEG_3$-nanotubes, did not disturb the electrostatic repulsion among the $GlcEG_3$-nanotubes. At pH 6, the $GlcEG_3$-nanotube dispersion failed to form liquid crystals and instead became turbid in the presence of Con A (which is positively charged at pH 6.0) owing to aggregation of the $GlcEG_3$-nanotubes caused by nonspecific adsorption of Con A (Fig. S8, ESI).

The $GlcEG_5$-nanotubes also formed a hydrogel at a relatively high Con A concentration (Fig. 3d, Con A = 80 nmol). In contrast, the dispersion scarcely responded to a relatively low concentration of Con A (Fig. 3d, Con A = 20 nmol), even though $GlcEG_5$ did form a complex with Con A; the higher flexibility of the long ethylene glycol chain in $GlcEG_5$ will prevent side-by-side alignment of the $GlcEG_5$-nanotubes (Fig. S9, ESI). The complexation of the $GlcEG_1$-nanotubes with Con A decreased the dispersibility of the nanotubes, and precipitates composed of the nanotubes and Con A formed (Fig. 3b). The length of the ethylene glycol unit in $GlcEG_1$ was insufficient for maintaining the dispersibility of the $GlcEG_1$-nanotubes complexed with Con A.

For naked-eye detection of Con A, the $GlcEG_3$-nanotube showed two-step responsiveness, that is, liquid crystal formation and hydrogel formation, depending on the concentration of Con A; in contrast, the $GlcEG_1$-nanotube and $GlcEG_5$-nanotube showed one-step responsiveness with precipitate formation and hydrogel formation, respectively (Fig. 3f). Therefore, the $GlcEG_3$-nanotube was superior to the other $GlcEG_n$-nanotubes in that it permitted semiquantitative detection of Con A.

The turbid hydrogel that was formed by complexation of the $GlcEG_3$-nanotubes with Con A broke down to a liquid crystal phase and then to a transparent solution in response to saccharides. The responsiveness and selectivity remarkably reflected the order of the association constants β (M^{-1}) for the interaction between the saccharides and Con A (Fig. 4): mannose (2.2×10^3) > glucose (8.0×10^2) >> galactose (which does not bind with Con A).[8]

In conclusion, we constructed soft nanotubes bearing recognition sites immobilized on the surface through ethylene glycol chains; the soft nanotubes organized hierarchically into a liquid crystal or a hydrogel depending on the concentration of the target analyte, Con A. Such a naked-eye detection system using two continuous macroscale changes has never been reported for conventional supramolecular hydrogels, which are capable of only one macroscale change (the sol–gel transition). Because soft nanotubes can be modified with recognition sites suitable for various target analytes, the system reported herein should open the way to the development not only of methods for on-site analysis and quick diagnosis without analytical instruments but also of analytical devices based on soft nanotube arrays.[3,10]

This work was partly supported by Grant-in-Aid for Scientific Research no. 26410107 from the Ministry of Education, Culture, Sports, Science and Technology of Japan.

Notes and references

[a] Nanosystem Research Institute (NRI), National Institute of Advanced Industrial Science and Technology (AIST), Tsukuba Central 5, 1-1-1 Higashi, Tsukuba, Ibaraki 305-8565, Japan.
E-mail: n-kameta@aist.go.jp; Fax: +81-29-861-4545; TEL: +81-29-861-4478
[b] AIST-Fellow

† Electronic Supplementary Information (ESI) available: Synthesis of $GlcEG_n$, TEM images of nanotubes and helical nanofibers, DSC profiles of fully hydrated nanotubes and helical nanofibers, IR spectra of lyophilized nanotubes, zeta-potential profiles of nanotubes, determination of association constants. See DOI: 10.1039/c000000x/

1 Recent reviews: (a) H. Jans, Q. Huo, *Chem. Rev. Soc.*, 2012, **41**, 2829; (b) K. Saha, S. S. Agasti, C. Kim, X. Li, V. M. Rotello, *Chem. Rev.*, 2012, **112**, 2739; (c) P. C. Ray, *Chem. Rev.*, 2010, **110**, 5332.

2 Recent reviews: (a) S. Fleming, R. V. Ulijn, *Chem. Rev. Soc.*, 2014, **43**, 8150; (b) C. Ren, J. Zhang, M. Chen, Z. Yang, *Chem. Soc. Rev.*, 2014, **43**, 7257; (c) X. Du, J. Zhou, B. Xu, *Chem. Asia. J.*, 2014, **9**, 1446; (d) J. Boekhoven, S. I. Stupp, *Adv. Mater.*, 2014, **26**, 1642; (e) E. M. White, J. Yatvin, J. B. Grubbs, J. A. Bilbrey, J. Locklin, *J. Polym. Sci. Part B Polym. Phys.*, 2013, **51**, 1084; (f) M. Yamanaka, *J. Incl. Phenom. Macrocycl. Chem.*, 2013, **77**, 33; (g) J. Liu, *Soft Matter*, 2011, **7**, 6757; (h) J. W. Steed, *Chem. Rev. Soc.*, 2010, **39**, 3686; (i) M. Ikeda, R. Ochi, I. Hamachi, *Lab Chip*, 2010, **10**, 3325; (j) P. Anzenbacher Jr, Y.-L. Liu, M. E. Kozelkova, *Curr. Opin. Chem. Biol.*, 2010, **14**, 693; (k) J. H. Jung, M. Park, S. Shinkai, *Chem. Soc. Rev.*, 2010, **39**, 4286.

3 Recent Reviews: (a) T. Shimizu, H. Minamikawa, M. Kogiso, M. Aoyagi, N. Kameta, W. Ding, M. Masuda, *Polym. J.*, 2014, **46**, 831; (b) T. G. Barclay, K. Constantopoulos, J. Matisons, *Chem. Rev.*, 2014, **114**, 10217; (c) S. S. Babu, V. K. Praveen, A. Ajayaghosh, *Chem. Rev.*, 2014, **114**, 1973; (d) J. P. Hill, L. K. Shrestha, S. Ishihara, Q. Ji, K. Ariga, *Molecules*, 2014, **19**, 8589; (e) Y. Kim, T. Kim, M. Lee, *Polym. Chem.*, 2013, **4**, 1300; (f) T. Aida, E. W. Meijer, S. I. Stupp, *Science*, 2012, **335**, 813.

4 (a) W. Ding, H. Minamikawa, N. Kameta, M. Wada, M. Masuda, T. Shimizu, *Langmuir*, 2015, **31**, 1150; (b) N. Kameta, K. Yoshida, M. Masuda, T. Shimizu, *Chem. Mater.*, 2009, **21**, 5892; (c) P. Terech, B. Jean, F. Ne, *Adv. Mater.*, 2006, **18**, 1571; (d) B. Jean, L. Oss-Ronen, P. Terech, Y. Talmon, *Adv. Mater.*, 2005, **17**, 728.

5 (a) N. Kameta, S. J. Lee, M. Masuda, *J. Mater. Chem. B*, 2013, **1**, 276; (b) N. Kameta, G. Mizuno, M. Masuda, H. Minamikawa, M. Kogiso, T. Shimizu, *Chem. Lett.*, 2007, **36**, 896.

6 T. Baba, L. Q. Zheng, H. Minamikawa, M. Hato, *J. Colloid Interface Sci.*, 2000, **223**, 235.

7 (a) Y. Sato, K. Yoshioka, T. Murakami, S. Yoshimito, O. Niwa, *Langmuir*, 2012, **28**, 1846; (b) Y. Sato, K. Yoshioka, M. Tanaka, T. Murakami, M. N. Ishida, O. Niwa, *Chem. Commun.*, 2008, 4909.

8 T. K. Dam, C. F. Brewer, *Chem. Rev.*, 2002, **102**, 387.

9 (a) M. H. Lu, C. Rosenblatt, *Mol. Cryst. Liq. Cryst.*, 1992, **210**, 169; (b) P. Yager, P. E. Schoen, *Mol. Cryst. Liq. Cryst.*, 1984, **106**, 371.

10 Recent reviews: (a) L. A. Abramovich, E. Gazit, *Chem. Soc. Rev.*, 2014, **43**, 6881; (b) R. de la Rica, H. Matsui, *Chem. Soc. Rev.*, 2010, **39**, 3499.